# SAR COMPLIANCE TESTING OF UNIDEN MODEL DATA 2000 CDPD MODEM

FINAL TECHNICAL REPORT

September 2, 1998

Submitted to:

Mr. Joseph W. Jackson
Communication Certification Laboratory
1940 West Alexander Street
West Valley City, Utah 84119

Submitted by:

Om P. Gandhi
Professor and Chairman
University of Utah
Electrical Engineering Department
50 S Central Campus Dr., Rm. 3280
Salt Lake City, UT 84112-9206

SAR COMPLIANCE TESTING OF UNIDEN MODEL
DATA 2000 CDPD MODEM

## I. Introduction

The U.S. Federal Communications Commission (FCC) has adopted limits of human exposure to RF emissions from mobile and portable devices that are regulated by the FCC [1]. The FCC has also recently issued Supplement C (Edition 97-01) to OET Bulletin 65 defining both the measurement and the computational procedures that should be followed for evaluating compliance of mobile and portable devices with FCC limits for human exposure to radiofrequency emissions [2].

For Uniden Model DATA 2000 CDPD Modem (FCC ID# AMWUH302), we have used the experimental measurement techniques to determine the SAR distributions from which the peak 1-g SARs are obtained for a variety of tilt angles of the antenna (0°, 45°, 90°, 135°, and 180°) relative to the base of the laptop modem (see e.g. Figs. 1a, b where the angles of the antenna relative to the base of the modem are 90° and 180°, respectively.) Since the modem is to be used in a laptop situation, a fiberglass model of the torso filled with a tissue-simulant medium is used for SAR measurements. This model, shown in Fig. 2, is mounted face down on the University of Utah Automated SAR Measurement Set Up [3]. As shown in Fig. 2, the modem is placed in contact with the model so that the radiating antenna is as close to the experimental model as possible.

## II. The Uniden Model DATA 2000 CDPD Modem

The Uniden Model DATA 2000 CDPD Modem (FCC ID# AMWUH302) operates in the frequency band 825-849 MHz for transmission frequencies (Channels 001-799). In the test mode, an internal attenuator can be adjusted for settings 0, 1, 2, ··· 10 with the power output being maximum for settings 0, 1, and 2 and decreasing monotonically to the lowest power levels for settings 8, 9, and 10 of the attenuator.

We have measured the power fed to the antenna by using a coaxial cable (measured insertion loss = 1.0 dB) which is connected to an output port provided for this purpose at the base of the radiating helix-monopole antenna of length 5 cm. The power output of the Uniden Model DATA 2000 CDPD Modem was measured at the low-frequency end (Channel 001, 825.03 MHz), at midband (Channel 383, 836.49 MHz) and at the high end (Channel 799, frequency 848.97 MHz), each for internal attenuator settings 0, 1, 2 ··· 10 by using Hewlett Packard (HP) Model 436A Power Meter with HP Model 8481 Power Sensor. After correcting for the coaxial cable loss of 1.0 dB, the measured variation of power output in dBm of this modem is given in Table 1. From Table l, it is interesting to note that the maximum power radiated at the high end (Channel 799, frequency = 848.97 MHz) is the rated 27.8 dBm (600 mW) while the radiated power is somewhat higher (by 0.4 dB) for the midband and the highest (1 dB higher) for the lowest radiating frequency (Channel 001, 825.03 MHz).

Even though the modem is recommended for operation with the antenna that is pulled up to be vertical (see Fig. 1a), it is recognized that a consumer may use the antenna for a variety of tilt angles from 0° (antenna left in its packing position) to 180° (see Fig. 1b) where the antenna is pulled out to be parallel to the base of the modem. It was, therefore, decided to make the SAR measurements for antenna tilt angles of 0°, 45°, 90°, 135°, and 180° at the center band frequency (Channel 383, frequency = 836.49 MHz) where 0° is the collapsed portable position of the antenna and 180° is the position where the antenna is completely pulled out (see Fig. 1b).

It was ascertained that the power output of the modem as measured at the output port at the base of the antenna is the same independent of the tilt angle of the antenna at the low end, midband, and at high-end transmission frequencies. Furthermore, the modem could be operated with no change in radiated power with the lid closed as shown in Figs. 1a, b. This was necessary so that the unit could be placed, as shown in Fig. 2, against the

torso model filled with the tissue-simulant fluid to probe the region of the highest SAR by inserting the E-field probe from the back side of the model.

We found that the battery life using four AA batteries was extremely limited and only on the order of 10-15 minutes when the wireless modem was operating at full power of 27.8 dBm (600 mW) and considerably longer if the unit was operated at a reduced power of 23.9 dBm (245 mW; attenuator setting of 3). It was, therefore, decided to make the SAR measurements for this reduced power setting and increase the SARs thus measured to the highest possible radiated power level of 600 mW (27.8 dBm) for the midband frequency.

## III. The Tissue-Simulant Model

The testing for the SAR distribution was done for the CDPD Modem mounted in contact with a fiberglass model of the human body shown in Fig. 2 which was placed face down with the back side cut for convenience of SAR measurements. The model was filled with a tissue-equivalent material simulating the average electromagnetic properties (dielectric constant $\varepsilon_r$ and electrical conductivity $\sigma$) for the lower torso region of the human body. This corresponds to $\varepsilon_r = 43.5$ and $\sigma = 0.9$ S/m for the CDPD Modem frequency of 825-849 MHz. For a composition of 40.4% water, 56.0% sugar, 2.5% salt (NaC$\ell$) and 1.0% HEC, we have measured the values of $\varepsilon_r = 41.1 \pm 1.4$ and $\sigma = 1.06 \pm 0.05$ S/m at 835 MHz using the HP Model 85070 B Dielectric Probe in conjunction with HP Model 8720 C Network Analyzer (50 MHz - 20 GHz). Since these values are very close to the desired values for $\varepsilon_r$ and $\sigma$, this composition was, therefore, used as the biological phantom material to fill the torso and the upper legs region of the model of the human body. The SAR distributions were measured using the automated 3-D stepper-motor driven SAR measurement system described in Appendix A [3]. To the extent that the conductivity $\sigma$ is slightly higher and the permittivity $\varepsilon_r$ is somewhat lower than the desired values, it should help in avoiding underestimating the SAR [2].

## IV. The E-Field Probe

The non-perturbing implantable E-field probe used in the SAR measuring system was originally developed by Bassen et al. [4] and is now manufactured by L3/Narda Microwave Corporation, Hauppauge, New York as Model 8021 E-field probe. In this probe, three orthogonal miniature dipoles are placed on a triangular beam substrate. Each dipole is loaded with a small Schottky diode and connected to the external circuitry by high resistance (2 MΩ ± 40%) leads to reduce secondary pickups. The entire structure is then encapsulated with a low dielectric constant insulating material. The probe thus constructed has a very small (4 mm) diameter, which results in a relatively small perturbation of the internal electric field.

### Test for Square Law Region

It is necessary to operate the E-field probe in the square law region for each of the diodes so that the sum of the dc voltage outputs from the three dipoles is proportional to the square of the internal electric field ($|E_i|^2$). Fortunately, the personal wireless devices induce SARs that are generally less than 5-6 W/kg even for closest locations of the model [5]. For compliance testing, it is, therefore, necessary that the E-field probe be checked for square law behavior for SARs up to such values that are likely to be encountered. Such a test may be conducted using a canonical lossy body such as a rectangular box or a sphere irradiated by a dipole. By varying the radiated power of the dipole, the output of the probe should increase linearly with the applied power for each of the test locations.

Shown in Figs. 3a, 3b are the results of the tests performed to check the square law behavior of the E-field probe used in our setup at 840 and 1900 MHz, respectively. For these measurements, we have used a rectangular box of dimensions 30 × 15 × 50 cm that was irradiated by the corresponding half wave dipoles with different amounts of radiated powers from 200-800 mW. Since the dc voltage outputs of the probe are fairly similar when normalized to a radiated power of 100 mW, the square law behavior is demonstrated and an output voltage that is proportional to $|E_i|^2$ is obtained within ± 3 percent.

### Test for Isotropy of the Probe

Another important characteristic of the probe that affects the measurement accuracy is its isotropy. Since the orientation of the induced electric field is generally unknown, the E-field probe should be relatively isotropic in its response to the orientation of the E-field. Shown in Figs. 4a, 4b are the test results of the E-field probe used in our setup at 840 and 1900 MHz, respectively. The previously described box phantom of dimensions $30 \times 15 \times 50$ cm along x, y and z dimensions, respectively, was also used for these measurements. This phantom was filled to a depth of 15 cm with brain-simulant materials (Table 2). The E-field probe was rotated around its axis from 0 to 360° in incremental steps of 60°. An isotropy of less than ± 0.23 dB (± 5.5%) was observed for this E-field probe both at 840 and 1900 MHz.

### Calibration of the E-Field Probe

Since the voltage output of the E-field probe is proportional to the square of the internal electric field ($|E_i|^2$), the SAR, given by $\sigma|E_i|^2/\rho$ is, therefore, proportional to the voltage output of the E-field probe by a proportionality constant C. The constant C is defined as the calibration factor, and is frequency and material dependent. It is measured to calibrate the probe at the various frequencies of interest using the appropriate tissue-simulating materials for the respective frequencies.

Canonical geometries such as waveguides, rectangular slabs and layered or homogeneous spheres have, in the past, been used for the calibration of the implantable E-field probe [6-8]. Since the Finite Difference Time Domain (FDTD) has been carefully validated to solve electromagnetic problems for a variety of geometries [9,10], we were able to calibrate the Narda E-field probe by comparing the measured variations of the probe voltage ($\approx |E_i|^2$) against the FDTD-calculated variations of SARs for a box phantom of dimensions $30 \times 15 \times 50$ cm used previously for the data given in Figs. 3 and 4, respectively. For these measurements, we placed the nominal half-wave dipoles of lengths 178 mm and 77 mm at 840 and 1900 MHz, respectively, at several distances d (see inserts

of Figs. 5a, 5b, and 6a, 6b) from the outer surface of the acrylic ($\varepsilon_r$ = 2.56) box of thickness 6.55 mm. Shown in Figs. 5a, 5b and 6a, 6b are the comparisons between the experimentally measured and FDTD-calculated variations of the SAR distributions for this box phantom. Since there are excellent agreements between the calculated SARs and the measured variations of the voltage output of the E-field probe for four different separations d of the half wave dipoles at each of the two frequencies, it is possible to calculate the calibration factors at the respective frequencies. For the Narda Model 8021 E-field probe used in our setup, the calibration factors are determined to be 0.49 and 0.84 (mW/kg)/μV at 840 and 1900 MHz, respectively.

## V. Experimental Results: Canonical Problems

To further validate the system, it has been used to measure the peak 1-g SAR for the above-mentioned box phantom and a glass sphere model of thickness 5 mm, external diameter = 223 mm and assumed dielectric constant $\varepsilon_r$ = 4.0. This sphere model is once again filled with the corresponding brain-simulant fluids of compositions given in Table 2. Shown in Figs. 7a, 7b and 8a, 8b are the measured and FDTD-calculated SAR distributions inside the sphere for various separations d between the dipole and the sphere (see insert for Figs. 7, 8). Comparison of the measured and FDTD-calculated peak 1-g SARs for both phantom geometries are given in Tables 3 and 4, respectively. As can be seen, the agreement between experimental measurement and numerical simulation is excellent and generally within ± 10 percent for both rectangular and spherical phantoms.

## VI. Measurement Uncertainty: Test Runs With Cellular Telephones

The automated setup shown in Fig. 2 of Appendix A has been used for the testing of ten personal wireless devices including some research test samples, five each at 835 and 1900 MHz, respectively. Given in Table 5 is the comparison of the numerical and measured peak 1-g SARs for these devices using our experimental phantom model and the

FDTD-based numerical procedure used for calculations of SAR distributions for an anatomically-based model of the head of an adult male [3]. The measured and calculated SARs for the ten telephones which have quite different operational modes (TDMA, CDMA, etc.) and antenna structures (helical, monopole, or helix-monopole) vary from 0.13 to 5.41 W/kg. Even though widely different peak 1-g SARs are obtained because of the variety of antennas and handsets, agreement between the calculated and the measured data is excellent and generally within ± 25%. This is particularly remarkable since an MRI-derived, 16-tissue anatomically-based model of the adult human head is used for FDTD calculations and a relatively simplistic two tissue phantom model is used for experimental peak 1-g SAR measurements.

We estimate the uncertainty of our measuring system to be ± 12.5 percent. As seen in Table 5, an agreement within ± 25 percent is obtained for the peak 1-g SARs calculated using the Utah FDTD Code and the Utah Experimental Phantom Model for ten assorted wireless devices using a variety of antennas and handset dimensions. Since both the numerical and experimental methods are completely independent methods, and each is prone to its own set of errors, an uncertainty of ± 12.5 percent can be ascribed to each of the methods.

## VII. The Measured SAR Distributions for Uniden Model DATA 2000 CDPD Modem

As shown in Fig. 2, the SAR distributions were measured for the Uniden Model DATA 2000 CDPD Modem mounted in contact with the torso region of the model. This model was filled with a tissue-equivalent material simulating the average electromagnetic properties ($\varepsilon_r$, $\sigma$) for the torso region of the human body (see Section III).

The highest SAR regions for each of the frequencies and antenna configurations vis à vis the model were determined in the first instance by using coarser sampling with a step size of 8.0 mm over three overlapping scan areas for a total scan area of $8.0 \times 9.6$ cm.

After identifying the region of the highest SAR for each of the cases, the SAR distributions were measured with a resolution of 2 mm in order to obtain the peak 1 $cm^3$ or 1-g SAR.

In Tables 6 and 7, we give the measured SAR distributions normalized to the maximum radiated power of 600 mW for the low end and midband frequencies of 825.03 and 836.49 MHz, respectively. For these measurements, the antenna was fully pulled out, as shown in Fig. 1b, to a tilt angle of 180°. As will be seen later in Tables 8-11, this is the configuration for the highest SAR. The peak 1-g SARs measured for this configuration of the antenna vis à vis the human body are 3.21 W/kg at 825.03 MHz (Channel 001) and 3.29 W/kg at the midband frequency of 836.49 MHz (Channel 383), respectively. These values are only 2.5 percent apart from each other i.e. well within the experimental errors involving the laptop placement, antenna tilt angle, etc.

Having thus demonstrated the relative lack of sensitivity to the radiation frequency, we made all subsequent measurements at the midband frequency of 836.49 MHz (Channel 383), but with different configuration angles of 0°, 45°, 90°, 135°, and 180° relative to the model of the torso where 0° is the collapsed portable position of the antenna and 90° and 180°, respectively, are the configurations of the antenna that is vertical (see Fig. 1a) and totally opened out and parallel to the surface of the model as in Fig. 1b. The SARs for the 0° configuration of the antenna were very low, generally, less than 0.1 W/kg, difficult to measure accurately, and are, therefore, not reported here. The SAR distributions measured with a step size of 2 mm for the highest SAR regions for 180°, 135°. 90°, and 45° orientations of the antenna are given in Tables 7-10, respectively. The peak 1-g SARs calculated for a maximum radiated power of 600 mW (27.8 dBm) for various configurations of the antenna are given in Table 11 and are 3.29, 2.04, 0.82, and 1.05 W/kg for antenna tilt angles of 180°, 135°, 90°, and 45° relative to the base of the modem, respectively.

## VIII. Comparison of the Data With FCC 96-326 Guidelines

According to the FCC 96-326 Guidelines [1], the peak SAR for any 1-g of tissue should not exceed 1.6 W/kg. As seen from Table 11, the 1-g SAR is less than 1.05 W/kg if antenna tilt angles less than 90° are used and are higher for angles in excess of 90° e.g. 135° and 180°. We, therefore, recommend a plastic built in retainer for the Uniden Model DATA 2000 CDPD Modem so that antenna angles larger than the vertical position of 90° would simply not be possible for this modem. This would allow the peak 1-g SAR to be less than the FCC 96-326 Guideline of 1.6 W/kg even at the low end transmission frequency where up to 1 dB larger radiated power of 28.8 dBm was measured as given in Table 1.

## REFERENCES


1. Federal Communications Commission, "Guidelines for Evaluating the Environmental Effects of Radiofrequency Radiation," FCC 96-326, August 1, 1996.

2. K. Chan, R. F. Cleveland, Jr., and D. L. Means, "Evaluating Compliance With FCC Guidelines for Human Exposure to Radiofrequency Electromagnetic Fields," Supplement C (Edition 97-01) to OET Bulletin 65, December, 1997. Available from Office of Engineering and Technology, Federal Communications Commission, Washington D.C., 20554.

3. Q. Yu, M.Aronsson, D. Wu, and O. P. Gandhi, "An Automated SAR Measurement System for Compliance Testing of Personal Wireless Devices," submitted to *IEEE Transactions on Electromagnetic Compatibility,* March 1998 (attached as Appendix A).

4. H. I. Bassen and G. S. Smith, "Electric Field Probes -- A Review," *IEEE Trans. Antennas Propagation*, Vol. 34, pp. 710-718, September 1983.

5. O. P. Gandhi, G. Lazzi and C. M. Furse, "Electromagnetic Absorption in the Human Head and Neck for Mobile Telephones at 835 and 1900 MHz," *IEEE Transactions on Microwave Theory and Techniques*, Vol. 44, pp. 1884-1897, 1996.

6. D. Hill, "Waveguide Techniques for the Calibration of Miniature Electric Field Probes for Use in Microwave Bioeffects Studies," *IEEE Trans. Microwave Theory Tech.,* Vol. 30, pp. 92-94, 1982.

7. N. Kuster and Q. Balzano, "Energy Absorption Mechanism by Biological Bodies in the Near Field of Dipole Antennas Above 300 MHz," *IEEE Trans. Veh. Technology,* Vol. 41, pp. 17-23, 1992.

8. M. A. Stuchly, S. S. Stuchly, and A. Kraszewski, "Implantable Electric Field Probes -- Some Performance Characteristics," *IEEE Trans. Biomed. Eng.,* Vol. 31, pp. 526-531, 1984.

9. A. Taflove, K. R. Umashankar, T. G. Jurgens, "Validation of FDTD Modeling of the Radar Cross Section of Three-Dimensional Structures Spanning Up to Nine Wavelengths," *IEEE Trans. Antennas and Propagation*, pp. 662-666, 1985.

10. C. M. Furse, Q. Yu, and O. P. Gandhi, "Validation of the Finite-Difference Time-Domain Method for Near-Field Bioelectromagnetic Simulations," *Microwave and Optical Technology Letters*, Vol. 16, pp. 341-345, 1997.

Table 1. The measured power output of the Uniden Model DATA 2000 CDPD Modem for different settings of the internal attenuator at low, midband, and high-end transmission frequencies.

| Attenuator Setting | Channel #001 f = 825.03 MHz | Channel #383 f = 836.49 MHz | Channel #799 f = 848.97 MHz |
|---|---|---|---|
| 0 | 28.8 | 28.2 | 27.8 |
| 1 | 28.8 | 28.2 | 27.8 |
| 2 | 28.8 | 28.2 | 27.8 |
| 3 | 24.8 | 23.9 | 23.8 |
| 4 | 21.1 | 20.1 | 20.0 |
| 5 | 17.5 | 16.4 | 16.3 |
| 6 | 14.1 | 13.0 | 12.9 |
| 7 | 9.0 | 8.0 | 7.5 |
| 8 | 9.0 | 8.0 | 7.5 |
| 9 | 9.0 | 8.0 | 7.5 |
| 10 | 9.0 | 8.0 | 7.5 |

Table 2. Compositions used for brain-equivalent materials.

| 840 MHz | | 1900 MHz | |
|---|---|---|---|
| Water | 40.4% | Water | 60.0% |
| Sugar | 56.0% | Sugar | 18.0% |
| Salt (NaCl) | 2.5% | PEP | 20.0% |
| HEC | 1.0% | Salt (NaCl) | 0.4% |
| | | TX 151 | 1.6% |
| $\varepsilon_r = 41.1 \pm 1.4$ | | $\varepsilon_r = 45.5 \pm 1.7$ | |
| $\sigma = 1.06 \pm 0.05$ S/m | | $\sigma = 1.31 \pm 0.06$ S/m | |

Table 3. Box phantom: Comparison of the measured and FDTD-calculated peak 1-g SARs for four spacings each at 840 and 1900 MHz, radiated power normalized to 0.5 W.

| Frequency (MHz) | Distance (mm) Between λ/2 Dipole and the Box | SAR (W/kg) | | Difference (%) |
|---|---|---|---|---|
| | | Measured | FDTD | |
| 840 | 17.5 | 4.58 | 4.20 | +8.3 |
| 840 | 22.5 | 3.53 | 3.65 | -3.4 |
| 840 | 27.5 | 2.69 | 3.00 | -10.2 |
| 840 | 33.0 | 1.95 | 2.24 | -12.9 |
| 1900 | 16.5 | 7.45 | 7.46 | -0.1 |
| 1900 | 21.5 | 4.24 | 4.18 | +1.4 |
| 1900 | 26.5 | 2.71 | 2.91 | -7.9 |
| 1900 | 31.5 | 1.77 | 1.75 | +1.1 |

Table 4. Sphere phantom: Comparison of the measured and FDTD-calculated peak 1-g SARs for three spacings each at 840 and 1900 MHz, radiated power normalized to 0.5 W.

| Frequency (MHz) | Distance (mm) Between λ/2 Dipole and the Box | SAR (W/kg) | | Difference (%) |
|---|---|---|---|---|
| | | Measured | FDTD | |
| 840 | 5 | 6.78 | 6.77 | +0.23 |
| 840 | 15 | 3.41 | 3.27 | +4.22 |
| 840 | 25 | 1.85 | 1.68 | +9.51 |
| 1900 | 5 | 17.45 | 18.01 | -3.21 |
| 1900 | 15 | 4.96 | 5.05 | -1.81 |
| 1900 | 25 | 1.69 | 1.77 | -4.73 |

Table 5. Comparison of the experimentally measured and FDTD-calculated peak 1-g SARs for ten wireless telephones, five each at 835 and 1900 MHz, respectively.

| | Time-Averaged Radiated Power mW | Using Experimental Model W/kg | Numerical Method W/kg |
|---|---|---|---|
| Cellular Telephones at 835 MHz | | | |
| Telephone A | 600 | 4.02 | 3.90 |
| Telephone B | 600 | 5.41 | 4.55 |
| Telephone C | 600 | 4.48 | 3.52 |
| Telephone D | 600 | 3.21 | 2.80 |
| Telephone E | 600 | 0.54 | 0.53 |
| PCS Telephones at 1900 MHz | | | |
| Telephone A′ | 125 | 1.48 | 1.47 |
| Telephone B′ | 125 | 0.13 | 0.15 |
| Telephone C′ | 125 | 0.65 | 0.81 |
| Telephone D′ | 125 | 1.32 | 1.56 |
| Telephone E′ | 99.3 | 1.41 | 1.25 |

Table 6. **The SARs measured for the CDPD Modem normalized to a radiated power of 600 mW (27.8 dBm) at the low-end frequency of 825.03 MHz. Antenna orientation of 180° relative to the model of the torso (see Fig. 1b).** The SARs in W/kg are measured with a step size of 2 mm for the highest SAR region of the model.

**1-g SAR** = 3.21 W/kg

**a. At depth of 1 mm**

| | | | | |
|---|---|---|---|---|
| 4.459 | 4.538 | 4.589 | 4.543 | 4.489 |
| 4.613 | 4.687 | 4.732 | 4.682 | 4.611 |
| 4.728 | 4.783 | 4.826 | 4.757 | 4.676 |
| 4.763 | 4.822 | 4.848 | 4.778 | 4.691 |
| 4.728 | 4.792 | 4.805 | 4.729 | 4.631 |

**b. At depth of 3 mm**

| | | | | |
|---|---|---|---|---|
| 3.601 | 3.666 | 3.706 | 3.677 | 3.637 |
| 3.721 | 3.783 | 3.818 | 3.786 | 3.735 |
| 3.810 | 3.861 | 3.893 | 3.849 | 3.789 |
| 3.841 | 3.890 | 3.913 | 3.864 | 3.799 |
| 3.813 | 3.864 | 3.879 | 3.824 | 3.751 |

**c. At depth of 5 mm**

| | | | | |
|---|---|---|---|---|
| 2.897 | 2.948 | 2.980 | 2.964 | 2.935 |
| 2.988 | 3.039 | 3.067 | 3.048 | 3.013 |
| 3.056 | 3.101 | 3.125 | 3.101 | 3.057 |
| 3.081 | 3.122 | 3.142 | 3.110 | 3.062 |
| 3.059 | 3.099 | 3.115 | 3.077 | 3.025 |

**d. At depth of 7 mm**

| | | | | |
|---|---|---|---|---|
| 2.346 | 2.387 | 2.411 | 2.405 | 2.385 |
| 2.415 | 2.456 | 2.478 | 2.469 | 2.445 |
| 2.464 | 2.504 | 2.523 | 2.510 | 2.481 |
| 2.484 | 2.518 | 2.535 | 2.516 | 2.482 |
| 2.465 | 2.498 | 2.514 | 2.489 | 2.452 |

**e. At depth of 9 mm**

| | | | | |
|---|---|---|---|---|
| 1.948 | 1.982 | 2.000 | 2.000 | 1.986 |
| 2.000 | 2.033 | 2.052 | 2.048 | 2.032 |
| 2.036 | 2.069 | 2.085 | 2.079 | 2.060 |
| 2.049 | 2.078 | 2.092 | 2.082 | 2.059 |
| 2.032 | 2.060 | 2.074 | 2.059 | 2.034 |

Table 7. **The SARs measured for the CDPD Modem normalized to a radiated power of 600 mW (27.8 dBm) at the midband frequency of 836.49 MHz. Antenna orientation of 180° relative to the model of the torso (see Fig. 1b).** The SARs in W/kg are measured with a step size of 2 mm for the highest SAR region of the model.

**1-g SAR** = 3.29 W/kg

**a. At depth of 1 mm**

| | | | | |
|---|---|---|---|---|
| 4.473 | 4.684 | 4.700 | 4.718 | 4.639 |
| 4.675 | 4.887 | 4.884 | 4.811 | 4.697 |
| 4.873 | 4.898 | 4.969 | 4.778 | 4.655 |
| 4.700 | 4.896 | 4.850 | 4.804 | 4.688 |
| 4.693 | 4.819 | 4.783 | 4.784 | 4.628 |

**b. At depth of 3 mm**

| | | | | |
|---|---|---|---|---|
| 3.735 | 3.817 | 3.838 | 3.836 | 3.788 |
| 3.822 | 3.960 | 3.947 | 3.910 | 3.817 |
| 3.947 | 3.972 | 3.996 | 3.890 | 3.799 |
| 3.818 | 3.939 | 3.934 | 3.915 | 3.838 |
| 3.818 | 3.903 | 3.878 | 3.894 | 3.796 |

**c. At depth of 5 mm**

| | | | | |
|---|---|---|---|---|
| 3.094 | 3.105 | 3.129 | 3.112 | 3.084 |
| 3.117 | 3.198 | 3.182 | 3.168 | 3.093 |
| 3.186 | 3.212 | 3.199 | 3.155 | 3.091 |
| 3.090 | 3.155 | 3.183 | 3.181 | 3.134 |
| 3.095 | 3.149 | 3.135 | 3.162 | 3.106 |

**d. At depth of 7 mm**

| | | | | |
|---|---|---|---|---|
| 2.551 | 2.545 | 2.569 | 2.546 | 2.527 |
| 2.561 | 2.602 | 2.588 | 2.587 | 2.527 |
| 2.589 | 2.619 | 2.578 | 2.571 | 2.531 |
| 2.517 | 2.544 | 2.596 | 2.601 | 2.575 |
| 2.524 | 2.557 | 2.555 | 2.589 | 2.559 |

**e. At depth of 9 mm**

| | | | | |
|---|---|---|---|---|
| 2.106 | 2.140 | 2.157 | 2.139 | 2.117 |
| 2.153 | 2.172 | 2.167 | 2.165 | 2.117 |
| 2.158 | 2.194 | 2.133 | 2.140 | 2.118 |
| 2.098 | 2.107 | 2.174 | 2.175 | 2.162 |
| 2.107 | 2.128 | 2.137 | 2.174 | 2.155 |

Table 8. **The SARs measured for the CDPD Modem normalized to a radiated power of 600 mW (27.8 dBm) at the midband frequency of 836.49 MHz. Antenna orientation of 135° relative to the model of the torso.** The SARs in W/kg are measured with a step size of 2 mm for the highest SAR region of the model.

**1-g SAR** = 2.04 W/kg

**a. At depth of 1 mm**

| | | | | |
|---|---|---|---|---|
| 2.853 | 2.888 | 2.893 | 2.875 | 2.837 |
| 2.925 | 2.954 | 2.946 | 2.917 | 2.857 |
| 2.971 | 3.002 | 2.997 | 2.956 | 2.885 |
| 2.993 | 3.015 | 3.003 | 2.948 | 2.862 |
| 2.964 | 2.998 | 2.987 | 2.916 | 2.822 |

**b. At depth of 3 mm**

| | | | | |
|---|---|---|---|---|
| 2.318 | 2.347 | 2.352 | 2.335 | 2.303 |
| 2.371 | 2.394 | 2.391 | 2.366 | 2.322 |
| 2.406 | 2.429 | 2.425 | 2.394 | 2.341 |
| 2.419 | 2.437 | 2.429 | 2.388 | 2.326 |
| 2.399 | 2.424 | 2.416 | 2.364 | 2.295 |

**c. At depth of 5 mm**

| | | | | |
|---|---|---|---|---|
| 1.888 | 1.911 | 1.915 | 1.900 | 1.873 |
| 1.925 | 1.944 | 1.944 | 1.923 | 1.891 |
| 1.951 | 1.969 | 1.966 | 1.942 | 1.903 |
| 1.957 | 1.972 | 1.966 | 1.937 | 1.894 |
| 1.944 | 1.962 | 1.955 | 1.920 | 1.869 |

**d. At depth of 7 mm**

| | | | | |
|---|---|---|---|---|
| 1.562 | 1.581 | 1.584 | 1.571 | 1.548 |
| 1.588 | 1.603 | 1.605 | 1.588 | 1.564 |
| 1.607 | 1.620 | 1.618 | 1.599 | 1.572 |
| 1.608 | 1.620 | 1.615 | 1.595 | 1.566 |
| 1.598 | 1.611 | 1.606 | 1.582 | 1.546 |

**e. At depth of 9 mm**

| | | | | |
|---|---|---|---|---|
| 1.341 | 1.355 | 1.358 | 1.348 | 1.329 |
| 1.360 | 1.371 | 1.373 | 1.360 | 1.342 |
| 1.372 | 1.382 | 1.381 | 1.367 | 1.346 |
| 1.371 | 1.380 | 1.377 | 1.362 | 1.342 |
| 1.362 | 1.371 | 1.368 | 1.351 | 1.324 |

Table 9. **The SARs measured for the CDPD Modem normalized to a radiated power of 600 mW (27.8 dBm) at the midband frequency of 836.49 MHz. Antenna orientation of 90° relative to the model of the torso (see Fig. 1a).** The SARs in W/kg are measured with a step size of 2 mm for the highest SAR region of the model.

**1-g SAR** = 0.82 W/kg

**a. At depth of 1 mm**

| | | | | |
|---|---|---|---|---|
| 1.169 | 1.185 | 1.189 | 1.176 | 1.187 |
| 1.197 | 1.210 | 1.205 | 1.188 | 1.171 |
| 1.205 | 1.214 | 1.218 | 1.195 | 1.192 |
| 1.204 | 1.223 | 1.216 | 1.207 | 1.181 |
| 1.229 | 1.214 | 1.212 | 1.198 | 1.180 |

**b. At depth of 3 mm**

| | | | | |
|---|---|---|---|---|
| 0.940 | 0.951 | 0.956 | 0.949 | 0.951 |
| 0.960 | 0.971 | 0.968 | 0.957 | 0.945 |
| 0.969 | 0.978 | 0.981 | 0.965 | 0.960 |
| 0.971 | 0.984 | 0.981 | 0.971 | 0.954 |
| 0.986 | 0.980 | 0.977 | 0.966 | 0.953 |

**c. At depth of 5 mm**

| | | | | |
|---|---|---|---|---|
| 0.751 | 0.760 | 0.765 | 0.762 | 0.759 |
| 0.766 | 0.775 | 0.774 | 0.769 | 0.760 |
| 0.776 | 0.784 | 0.785 | 0.776 | 0.769 |
| 0.779 | 0.788 | 0.787 | 0.778 | 0.768 |
| 0.787 | 0.787 | 0.784 | 0.776 | 0.766 |

**d. At depth of 7 mm**

| | | | | |
|---|---|---|---|---|
| 0.605 | 0.612 | 0.616 | 0.616 | 0.610 |
| 0.616 | 0.623 | 0.623 | 0.621 | 0.615 |
| 0.624 | 0.632 | 0.632 | 0.628 | 0.620 |
| 0.628 | 0.633 | 0.635 | 0.627 | 0.621 |
| 0.631 | 0.634 | 0.632 | 0.627 | 0.620 |

**e. Atdepth of 9 mm**

| | | | | |
|---|---|---|---|---|
| 0.500 | 0.506 | 0.509 | 0.511 | 0.505 |
| 0.508 | 0.514 | 0.514 | 0.515 | 0.510 |
| 0.514 | 0.521 | 0.522 | 0.520 | 0.512 |
| 0.518 | 0.521 | 0.524 | 0.519 | 0.515 |
| 0.518 | 0.523 | 0.521 | 0.518 | 0.515 |

Table 10. **The SARs measured for the CDPD Modem normalized to a radiated power of 600 mW (27.8 dBm) at the midband frequency of 836.49 MHz. Antenna orientation of 45° relative to the model of the torso.** The SARs in W/kg are measured with a step size of 2 mm for the highest SAR region of the model.

**1-g SAR** = 1.05 W/kg

**a. At depth of 1 mm**

| | | | | |
|---|---|---|---|---|
| 1.461 | 1.428 | 1.452 | 1.449 | 1.494 |
| 1.445 | 1.497 | 1.473 | 1.473 | 1.488 |
| 1.467 | 1.461 | 1.473 | 1.469 | 1.480 |
| 1.443 | 1.453 | 1.451 | 1.452 | 1.439 |
| 1.422 | 1.437 | 1.494 | 1.515 | 1.442 |

**b. At depth of 3 mm**

| | | | | |
|---|---|---|---|---|
| 1.206 | 1.188 | 1.208 | 1.203 | 1.222 |
| 1.201 | 1.230 | 1.220 | 1.219 | 1.221 |
| 1.213 | 1.212 | 1.220 | 1.218 | 1.218 |
| 1.197 | 1.205 | 1.203 | 1.202 | 1.189 |
| 1.185 | 1.196 | 1.229 | 1.242 | 1.188 |

**c. At depth of 5 mm**

| | | | | |
|---|---|---|---|---|
| 1.000 | 0.993 | 1.010 | 1.003 | 1.002 |
| 1.004 | 1.016 | 1.016 | 1.013 | 1.006 |
| 1.008 | 1.011 | 1.016 | 1.014 | 1.005 |
| 0.998 | 1.004 | 1.002 | 0.999 | 0.986 |
| 0.992 | 1.000 | 1.016 | 1.020 | 0.983 |

**d. At depth of 7 mm**

| | | | | |
|---|---|---|---|---|
| 0.844 | 0.843 | 0.857 | 0.849 | 0.834 |
| 0.852 | 0.853 | 0.859 | 0.854 | 0.841 |
| 0.852 | 0.857 | 0.859 | 0.856 | 0.842 |
| 0.846 | 0.850 | 0.848 | 0.842 | 0.829 |
| 0.843 | 0.849 | 0.853 | 0.851 | 0.826 |

**e. At depth of 9 mm**

| | | | | |
|---|---|---|---|---|
| 0.735 | 0.739 | 0.750 | 0.741 | 0.718 |
| 0.746 | 0.743 | 0.749 | 0.744 | 0.728 |
| 0.744 | 0.749 | 0.749 | 0.746 | 0.729 |
| 0.740 | 0.743 | 0.740 | 0.731 | 0.719 |
| 0.739 | 0.742 | 0.742 | 0.732 | 0.718 |

Table 11. Summary of the measured peak 1-g SARs for the Uniden Model DATA 2000 CDPD Modem for a maximum radiated power of 600 mW (27.8 dBm) at the midband frequency of 836.49 MHz (Channel 383) for various tilt angles of the antenna relative to the model of the torso.

| Antenna Tilt Angle | Table | Peak 1-g SAR W/kg |
|---|---|---|
| 0° | -- | < 0.1* |
| 45° | 10 | 1.05 |
| 90° (see Fig. 1a) | 9 | 0.82 |
| 135° | 8 | 2.04 |
| 180° (see Fig. 1b) | 7 | 3.29 |

* Too low to measure accurately.

(a)

(b)

Fig. 1. Photograph of the Uniden Model DATA 2000 CDPD Modem with two representative orientations of the antenna.

a. Antenna vertical at an angle of 90° relative to the base of the modem.

b. Antenna completely pulled out i.e. at an angle of 180° relative to the collapsed portable position (called 0°)

Fig. 2. The phantom model used for determination of SARs due to the CDPD Modem. The model is filled with tissue-simulant fluid and turned upside down to probe the region of the highest SAR by inserting the E-field probe from the back side of the model.

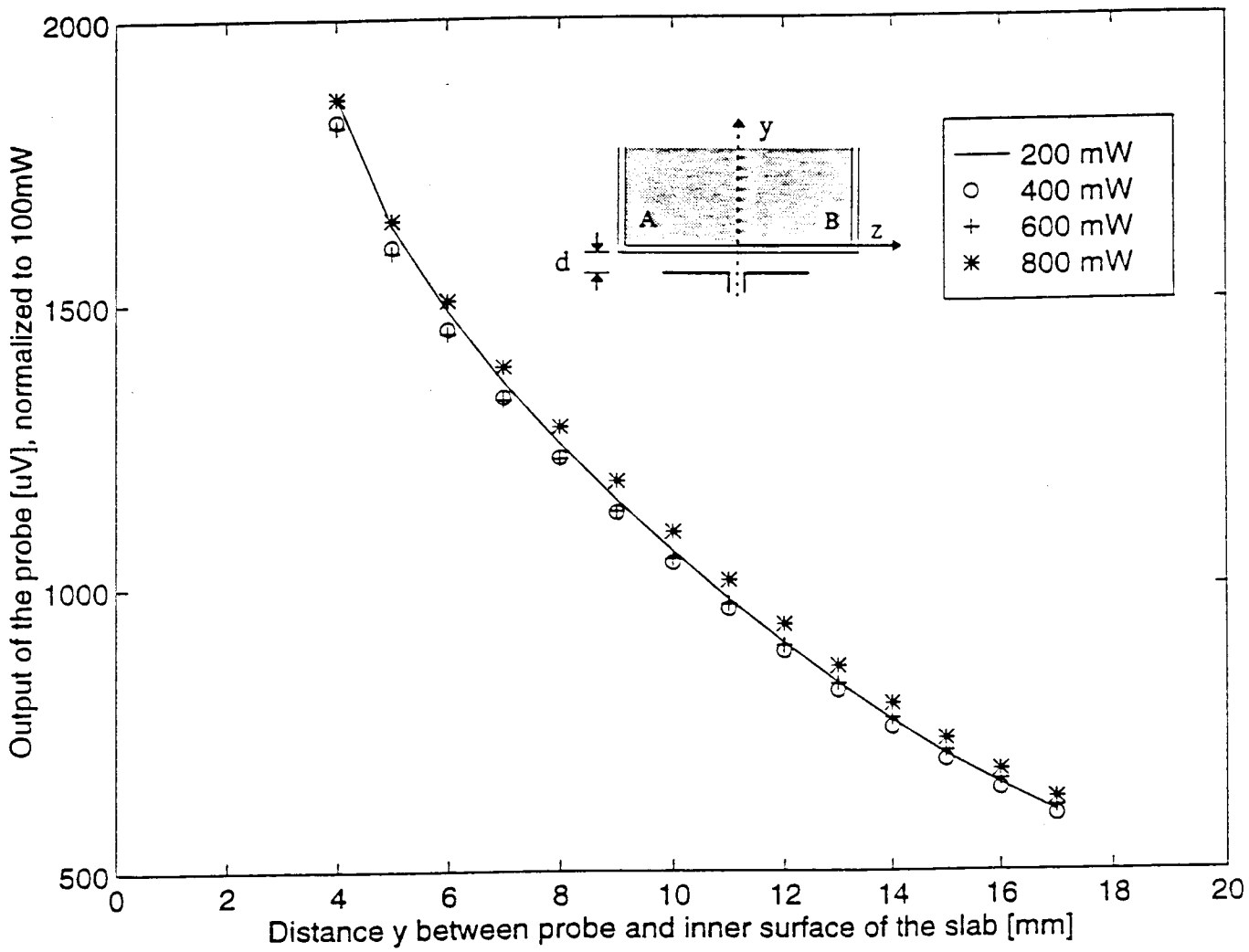


Fig. 3a. Test for square-law behavior at 840 MHz: Variation of the output voltage (proportional to $|E_i|^{2)}$ for different radiated powers normalized to 0.1 W.

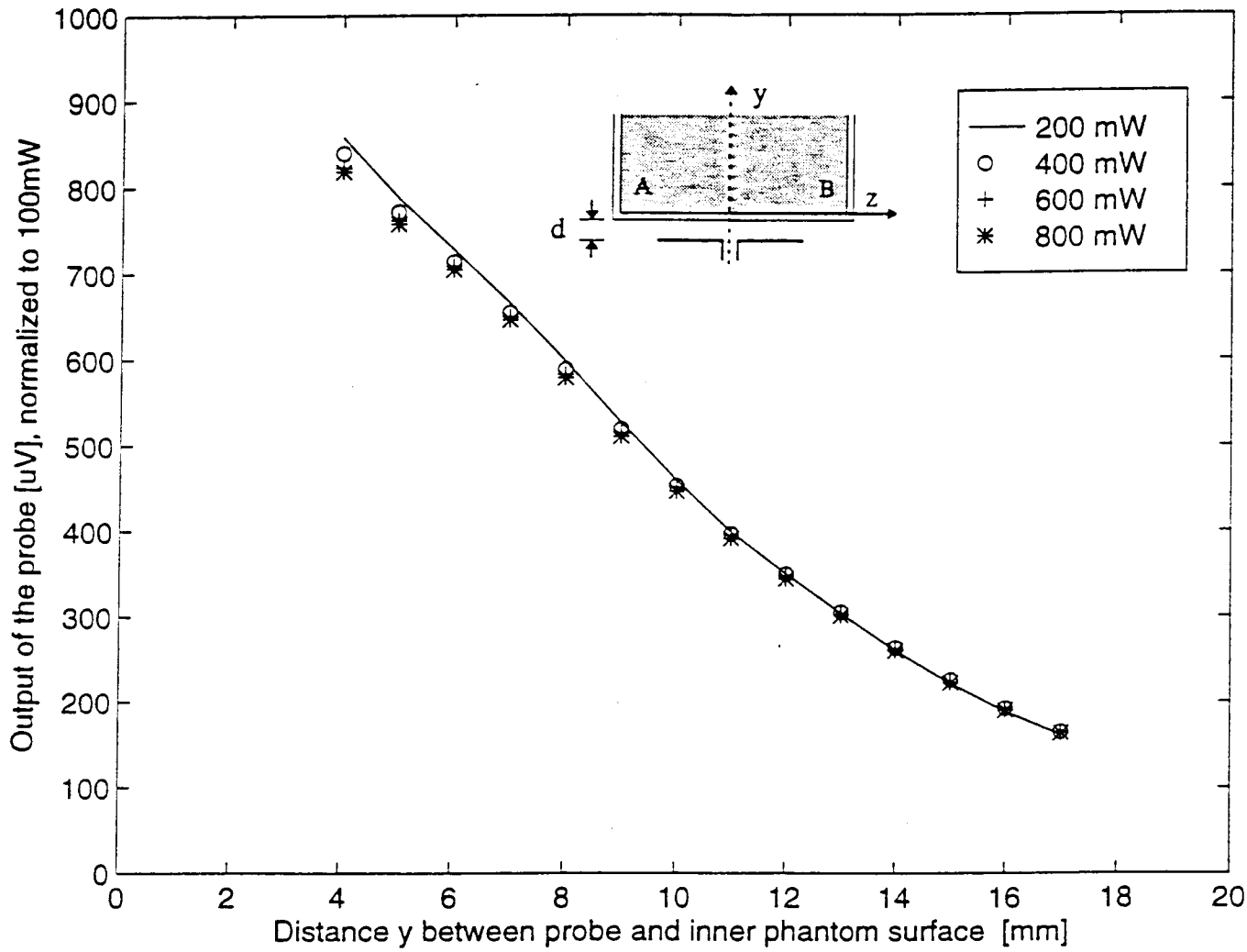


Fig. 3b. Test for square-law behavior at 1900 MHz: Variation of the output voltage (proportional to $|E_i|^{(2)}$ for different radiated powers normalized to 0.1 W.

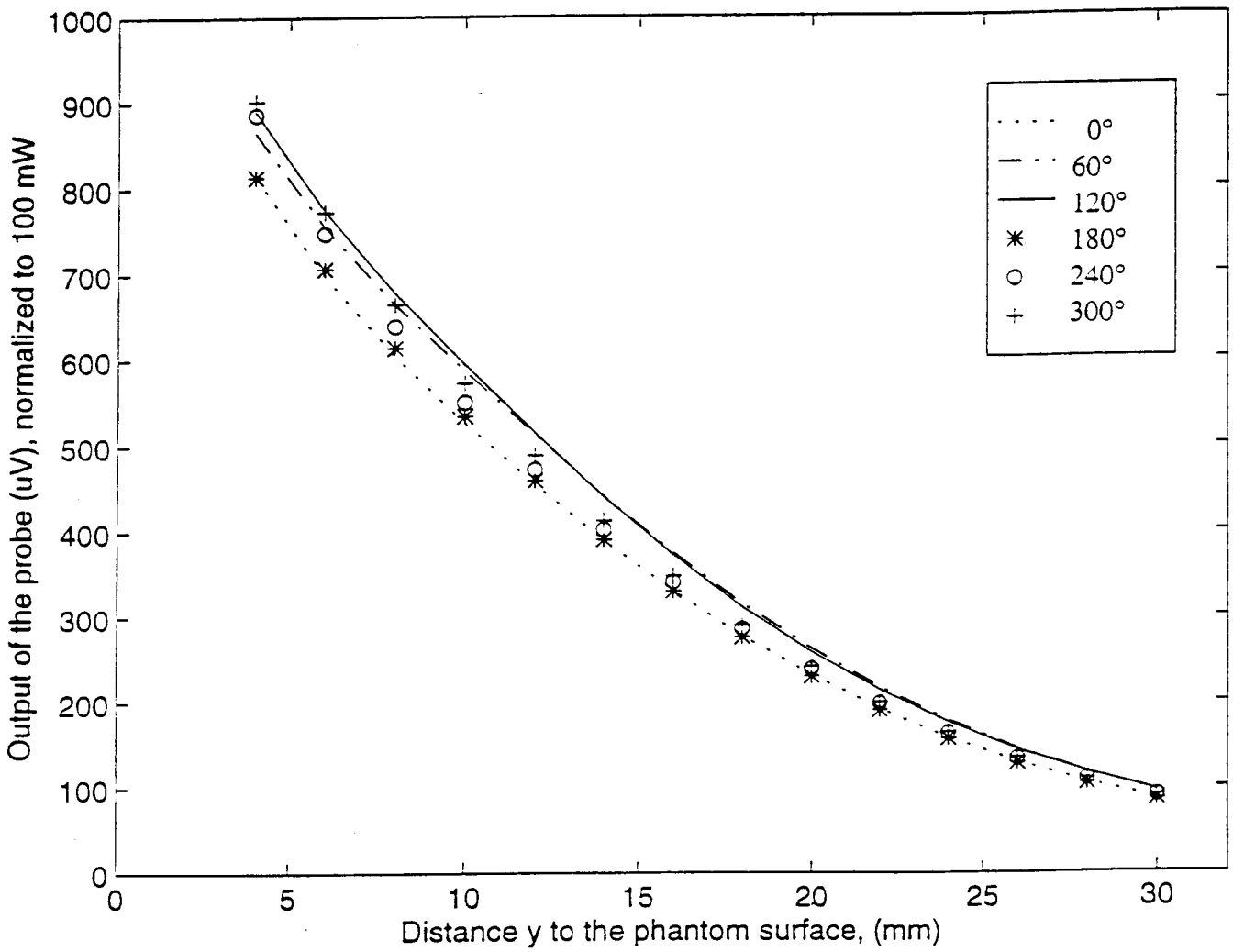


Fig. 4a. Test for isotropy: The model shown in Fig. 2 was used with nominal half wavelength dipole radiator of length 178 mm at 840 MHz.

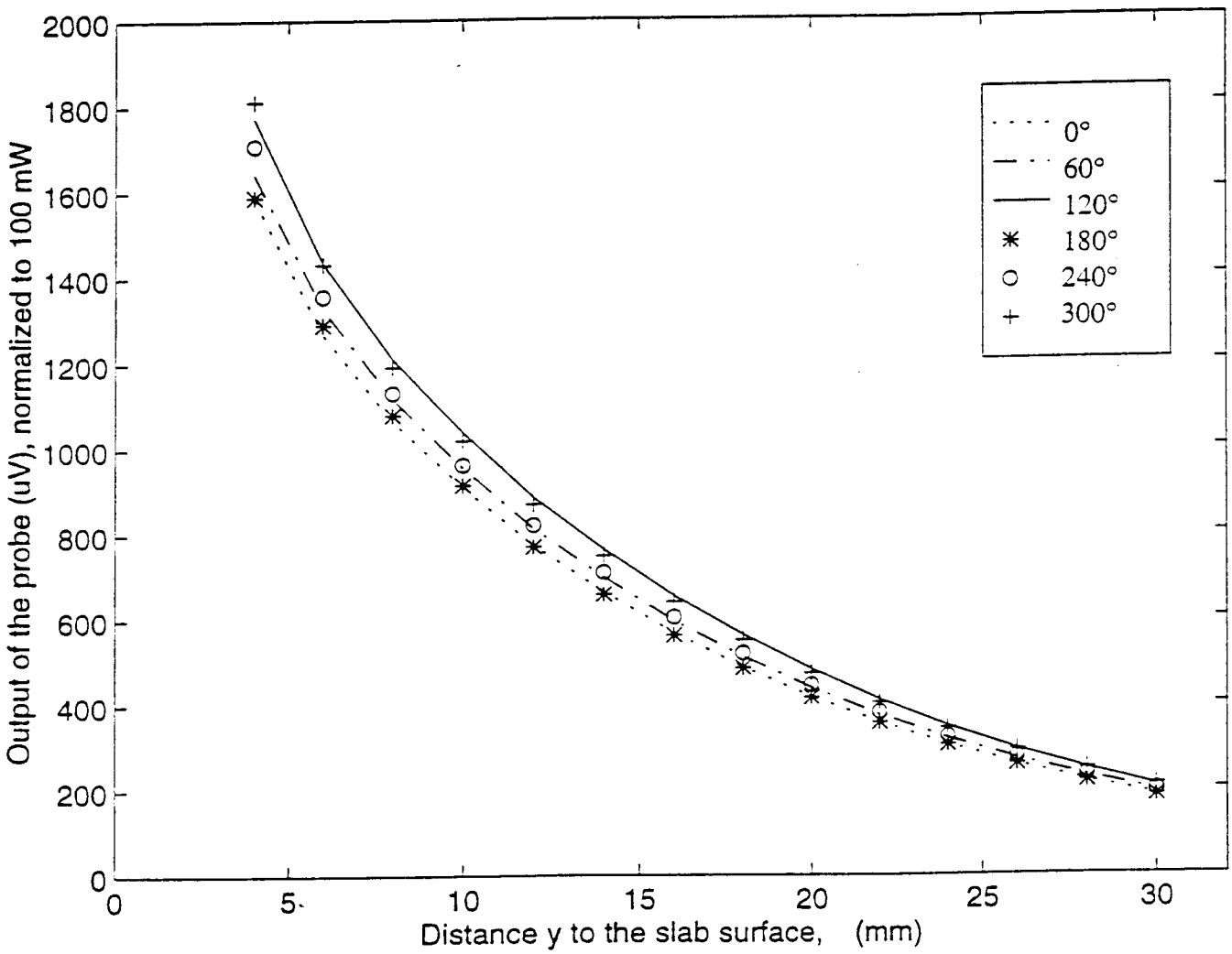


Fig. 4b. Test for isotropy: The model shown in Fig. 2 was used with nominal half wavelength dipole radiator of length 77 mm at 1900 MHz.

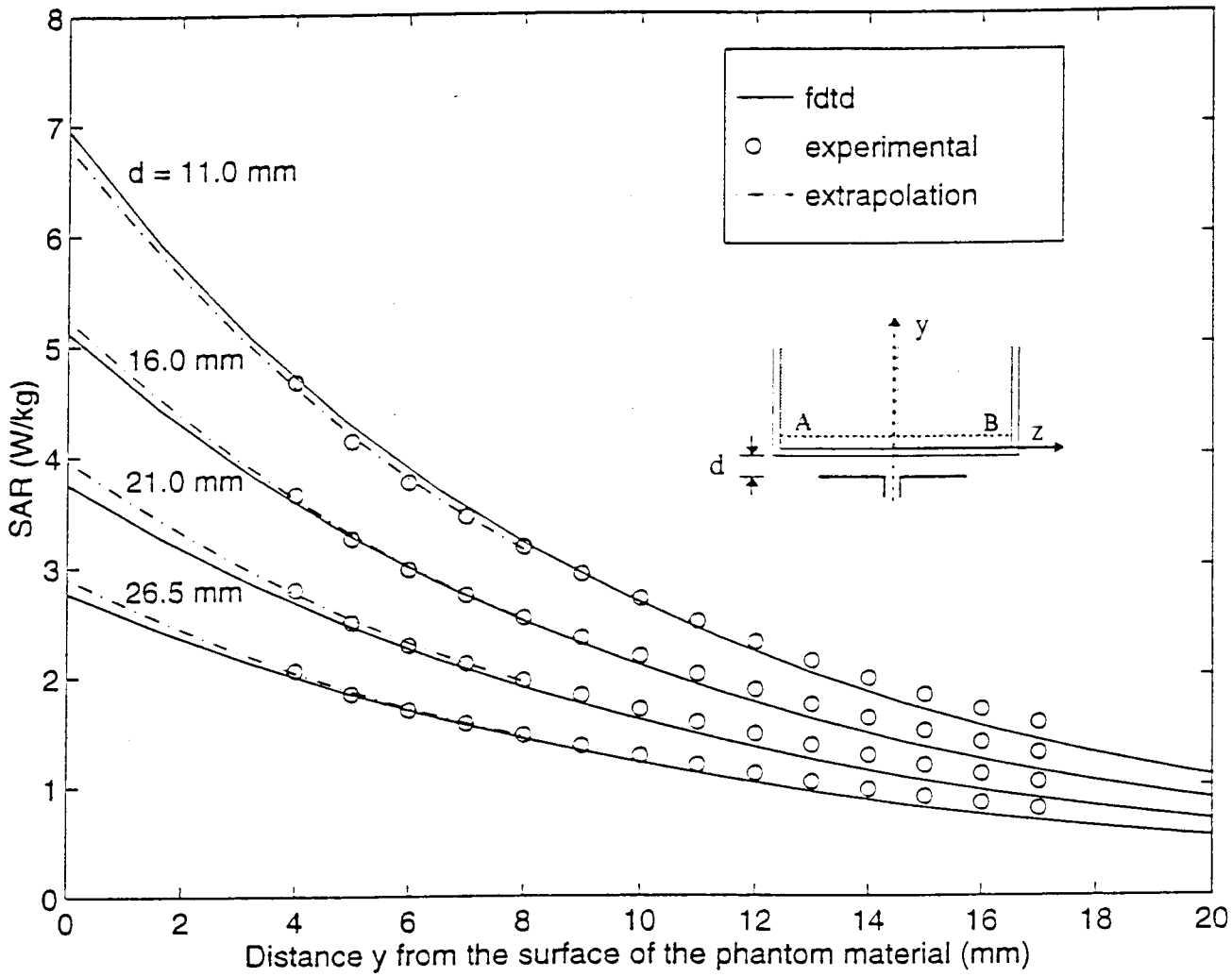


Fig. 5a. Comparison of the calculated and measured SAR variations for a box phantom of dimensions 30 × 15 × 50 cm; 840 MHz; $\lambda/2$ dipole antenna; 0.5 W radiated power. Calibration factor for the Narda Model 8021 probe at 840 MHz = 0.49 (mW/kg)/$\mu$V. Measured for the phantom material $\varepsilon_r = 41.1$, $\sigma = 1.06$ S/m.

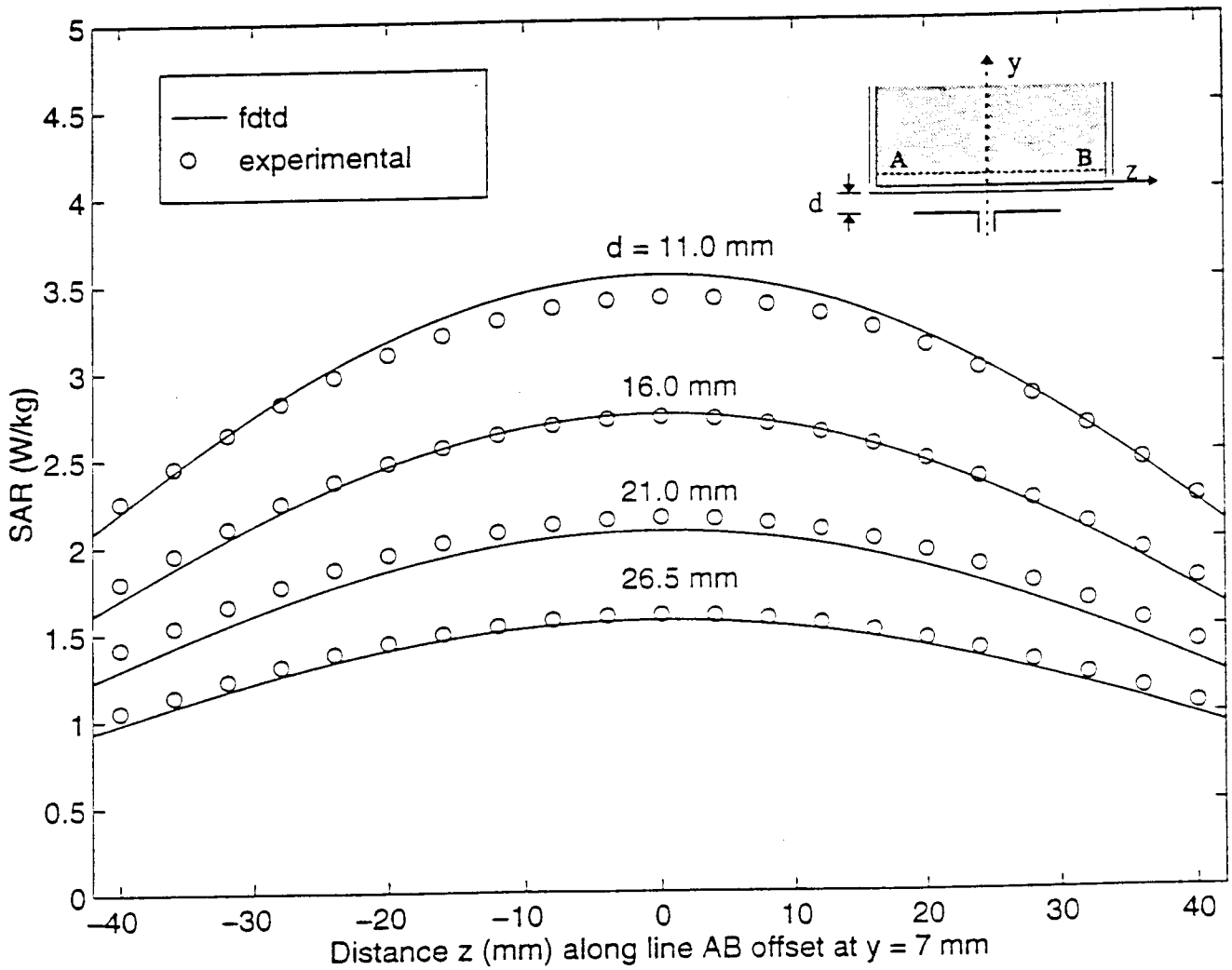


Fig. 5b. Comparison of the calculated and measured SAR variations for a box phantom of dimensions $30 \times 15 \times 50$ cm for a line AB parallel to the z axis at a distance y = 7 mm from the surface of the phantom material; 840 MHz; $\lambda/2$ dipole antenna; 0.5 W radiated power. Calibration factor for the Narda Model 8021 probe at 840 MHz = 0.49 (mW/kg)/μV. Measured for the phantom material $\varepsilon_r = 41.1$, $\sigma = 1.06$ S/m.

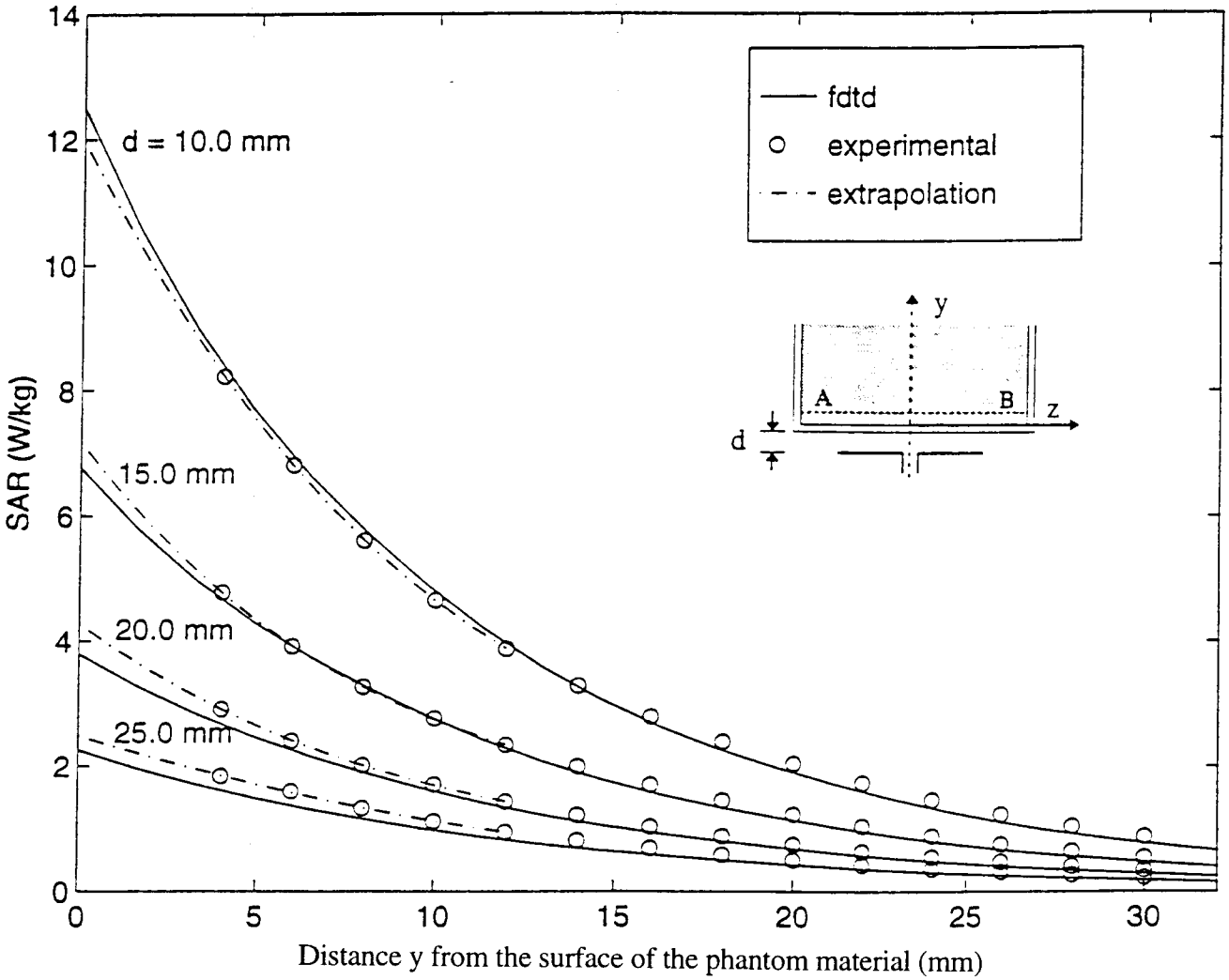


Fig. 6a. Comparison of the calculated and measured SAR variations for a box phantom of dimensions 30 × 15 × 50 cm; 1900 MHz; λ/2 dipole antenna; 0.5 W radiated power. Calibration factor for the Narda Model 8021 probe at 1900 MHz = 0.84 (mW/kg)/μV. Measured for the phantom material $\varepsilon_r = 45.5$, $\sigma = 1.31$ S/m.

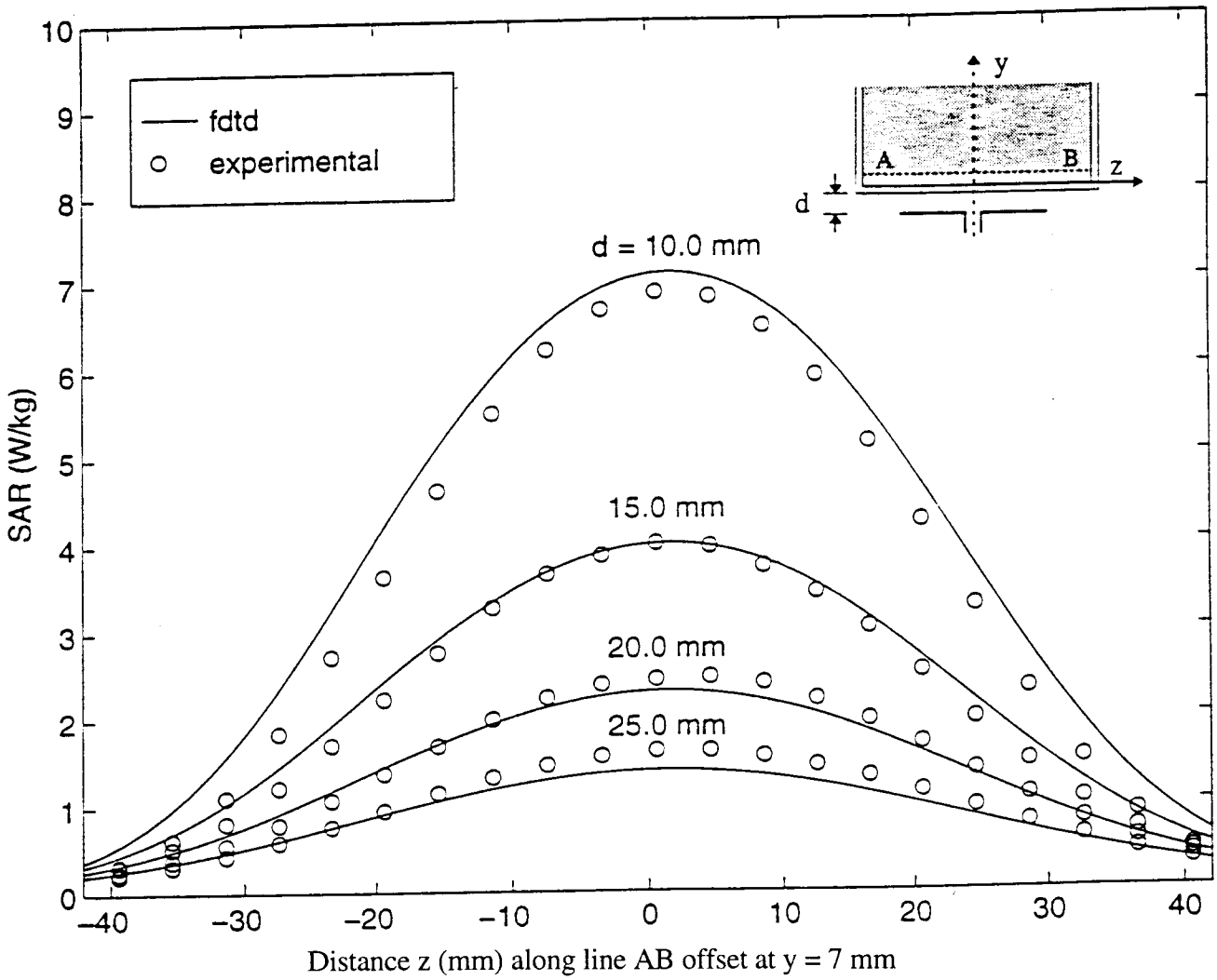


Fig. 6b. Comparison of the calculated and measured SAR variations for a box phantom of dimensions $30 \times 15 \times 50$ cm for a line AB parallel to the z axis at a distance y = 7 mm from the surface of the phantom material; 1900 MHz; $\lambda/2$ dipole antenna; 0.5 W radiated power. Calibration factor for the Narda Model 8021 probe at 1900 MHz = 0.84 (mW/kg)/$\mu$V. Measured for the phantom material $\varepsilon_r = 45.5$, $\sigma = 1.31$ S/m.

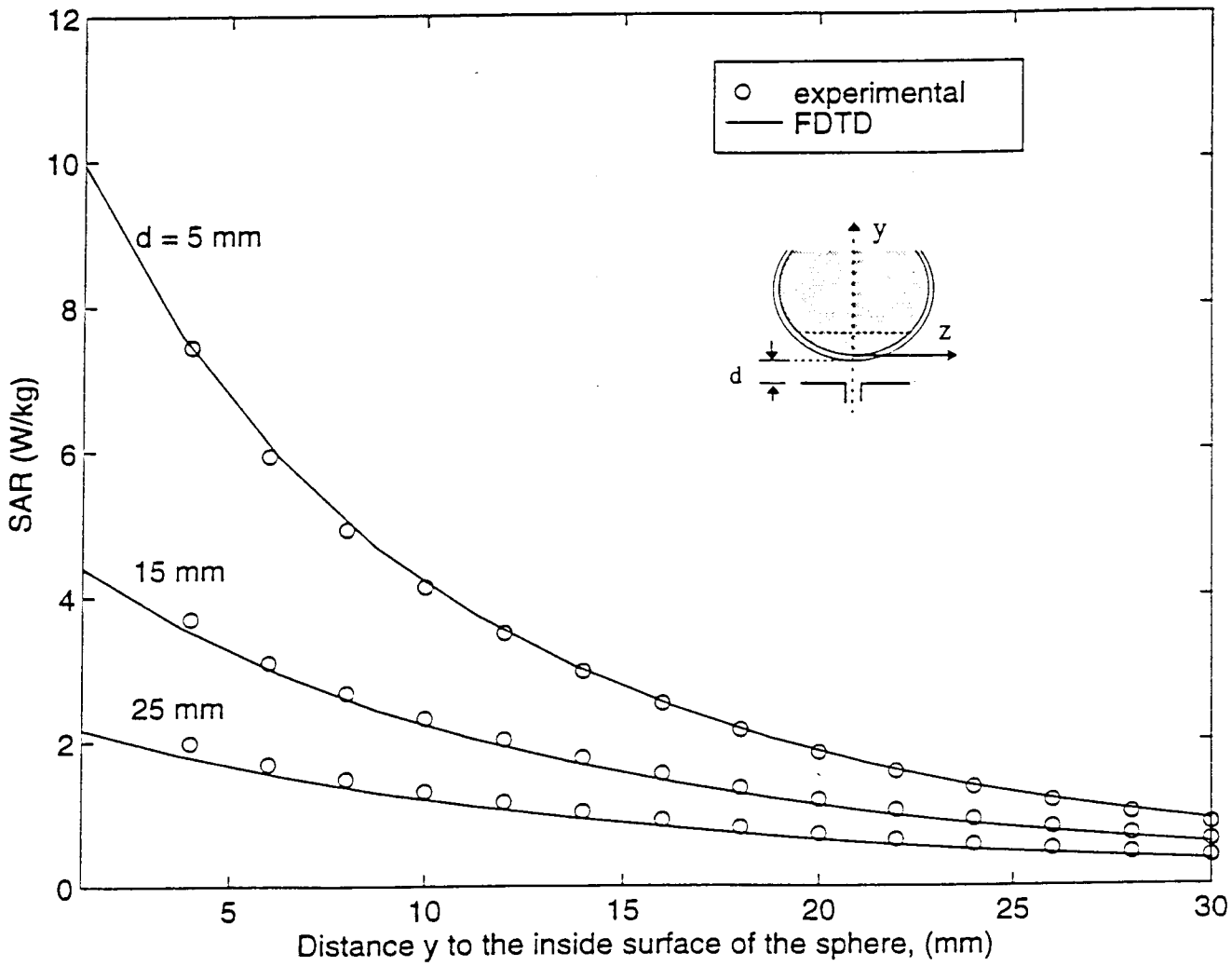


Fig. 7a. Comparison of measured and FDTD-calculated SAR variations at 840 MHz for a glass sphere model of outer diameter 22.3 cm and thickness 5 mm. SARs normalized to a radiated power of 0.5 W. Calibration factor = 0.49 (mW/kg)/μV. Measured for the phantom material $\varepsilon_r = 41.1$, $\sigma = 1.06$ S/m.

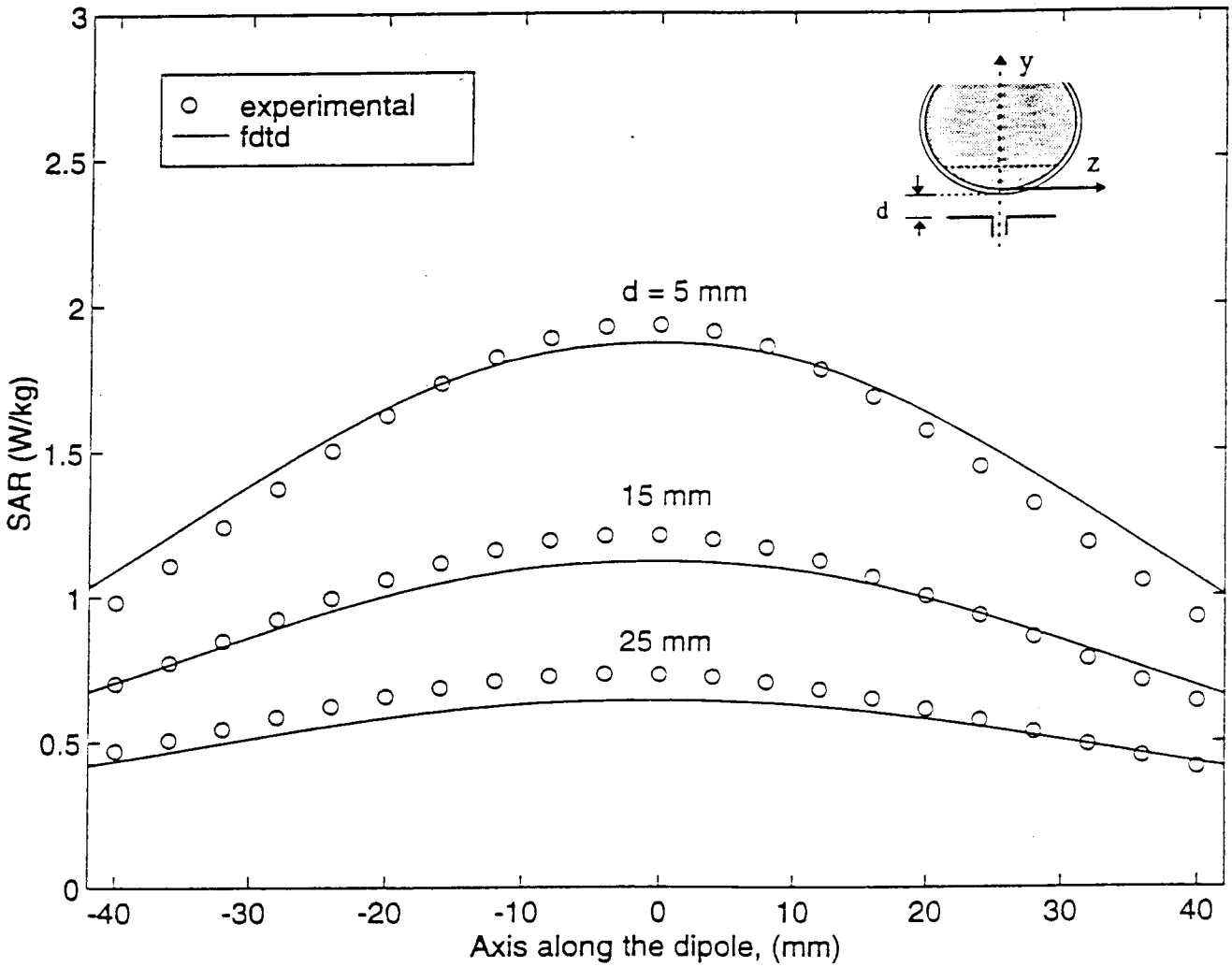


Fig. 7b. Comparison of calculated and measured SAR variations at 840 MHz for a plane at a distance of 20 mm from the lowest point on the inside of the sphere. SARs normalized to a radiated power of 0.5 W. Calibration factor = 0.49 (mW/kg)/μV. Measured for the phantom material $\varepsilon_r = 41.1$, $\sigma = 1.06$ S/m.

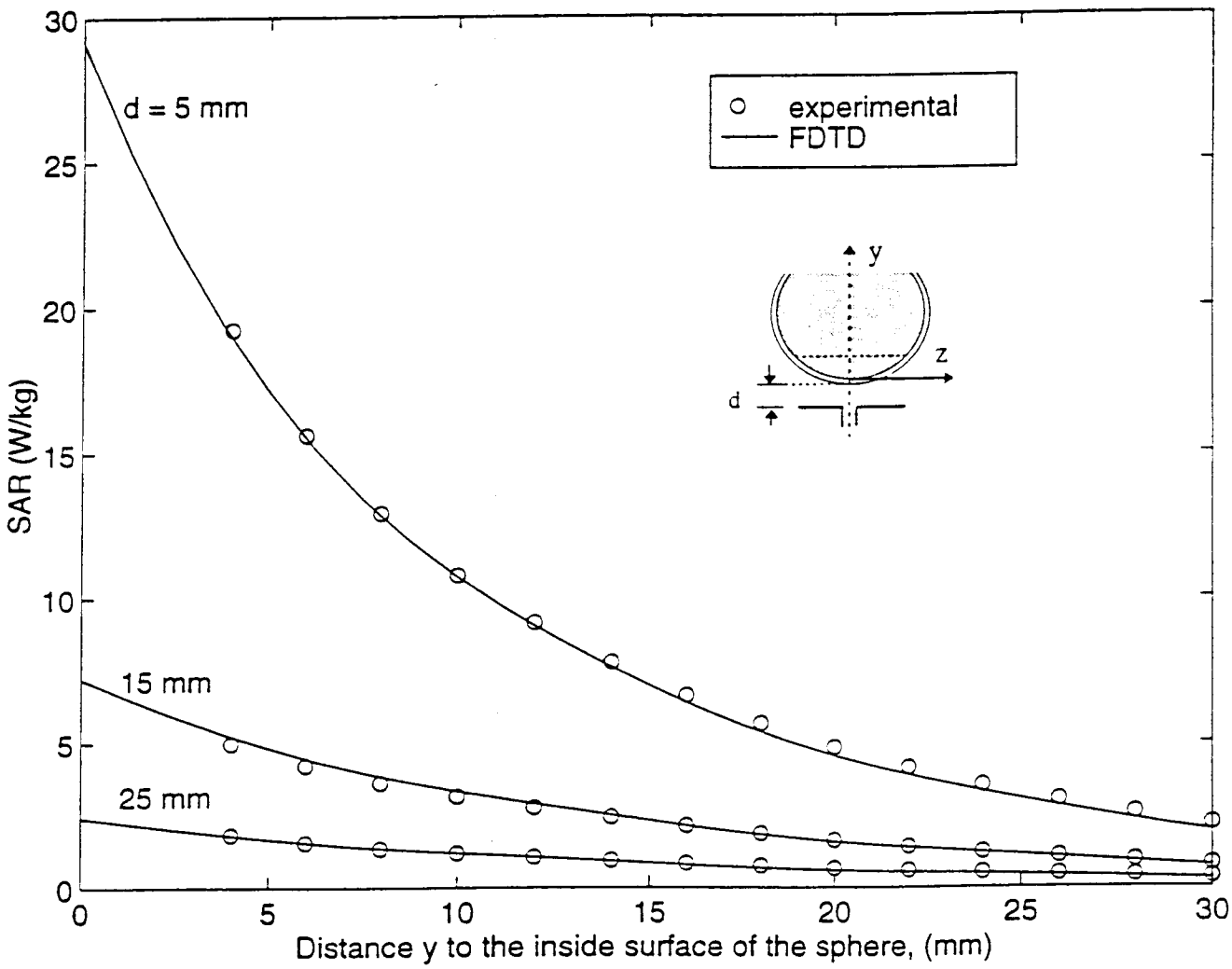


Fig. 8a. Comparison of measured and FDTD-calculated SAR variations at 1900 MHz for a glass sphere model of outer diameter 22.3 cm and thickness 5 mm. SARs normalized to a radiated power of 0.5 W. Calibration factor = 0.84 (mW/kg)/μV. Measured for the phantom material $\varepsilon_r = 45.5$, $\sigma = 1.31$ S/m.

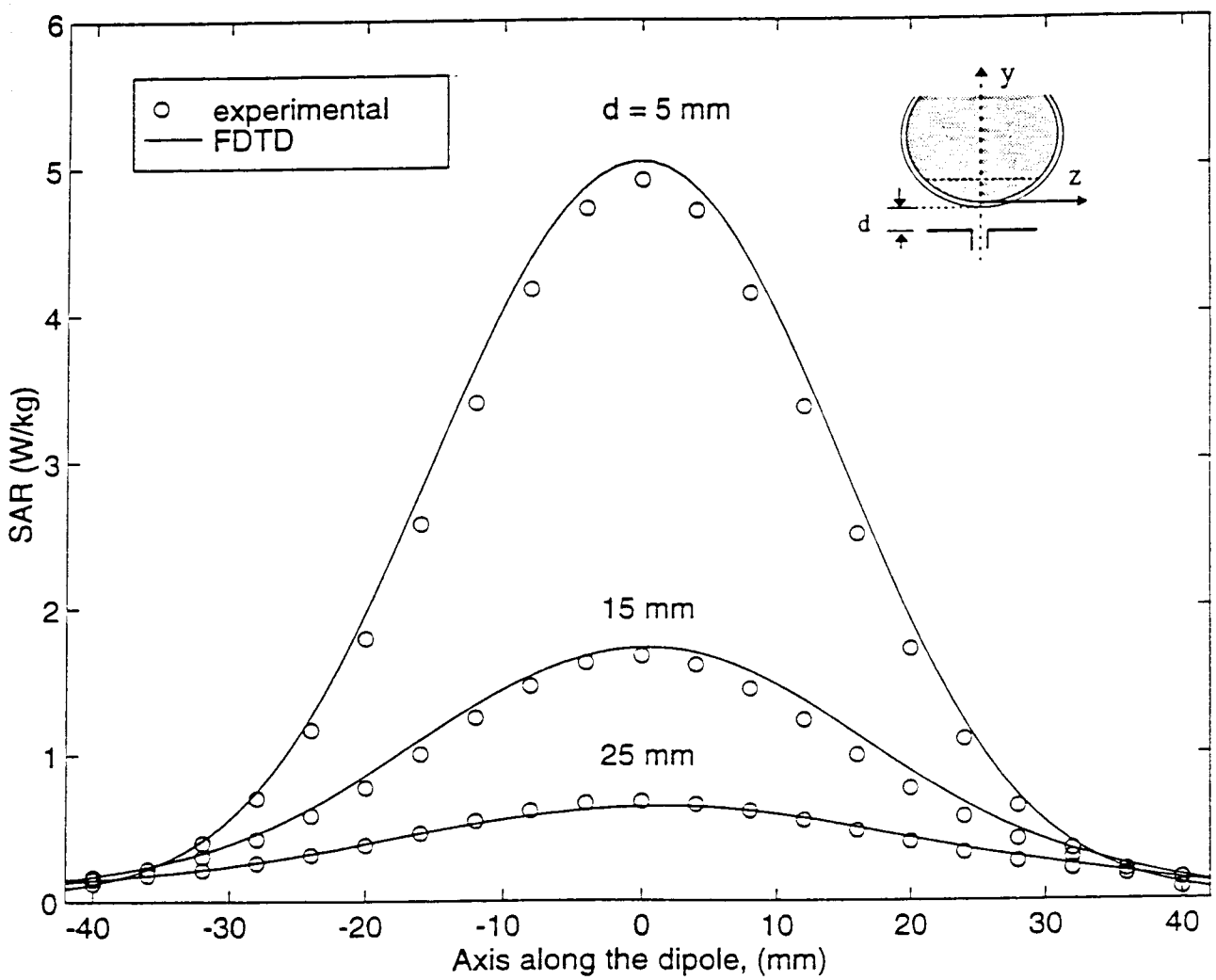


Fig. 8b. Comparison of calculated and measured SAR variations at 1900 MHz for a plane at a distance of 20 mm from the lowest point on the inside of the sphere. SARs normalized to a radiated power of 0.5 W. Calibration factor = 0.84 (mW/kg)/μV. Measured for the phantom material $\varepsilon_r = 45.5$, $\sigma = 1.31$ S/m.